View metadata, citation and similar papers at core.ac.uk

brought to you by CORE

provided by NASA Technical Reports Server

General Disclaimer

One or more of the Following Statements may affect this Document

- This document has been reproduced from the best copy furnished by the organizational source. It is being released in the interest of making available as much information as possible.

- This document may contain data, which exceeds the sheet parameters. It was furnished in this condition by the organizational source and is the best copy available.

- This document may contain tone-on-tone or color graphs, charts and/or pictures, which have been reproduced in black and white.

- This document is paginated as submitted by the original source.

- Portions of this document are not fully legible due to the historical nature of some of the material. However, it is the best reproduction available from the original submission.

Produced by the NASA Center for Aerospace Information (CASI)

(NASA-TM-80329) THE DIFFUSE X-RAY BACKGROUND SPECTRUM FROM 3 TO 50keV (NASA) 25 p HC A02/MF A01 CSCL 03B

N79-31132

Unclas
G3/93 36074

NASA

Technical Memorandum **80329**

The Diffuse X-Ray Background Spectrum from 3 to 50 keV

**F. E. Marshall, E. A. Boldt,
S. S. Holt, R. Miller,
R. F. Mushotzky, L. A. Rose,
R. E. Rothschild and P. J. Serlemitsos**

JULY 1979

National Aeronautics and
Space Administration

Goddard Space Flight Center
Greenbelt, Maryland 20771

THE DIFFUSE X-RAY BACKGROUND SPECTRUM FROM 3 to 50 keV

F.E. Marshall*, E.A. Boldt, S.S. Holt, R. Miller**, R.F. Mushotzky*, L.A. Rose*, R.E. Rothschild***, and P.J. Serlemitsos

Laboratory for High Energy Astrophysics
NASA/Goddard Space Flight Center
Greenbelt, Maryland 20771 USA

ABSTRACT

The spectrum of the extragalactic diffuse X-ray background has been measured with the GSFC Cosmic X-Ray Experiment on HEAO-1 for regions of the sky away from known point sources and more than 20^{0} from the galactic plane. A total exposure of 80 m^2-sec-sr is available at present. Free-free emission from an optically thin plasma of 40 $\pm$ 5 keV provides an excellent description of the observed spectrum from 3 to 50 keV. This spectral shape is confirmed by measurements from 5 separate layers of three independent detectors. With an estimated absolute precision of $\sim$ 10%, the intensity of the emission at 10 keV is 3.2 keV/keV-cm^2-sec-sr, a value consistent with the average of previously reported spectra. No other spectral features, such as iron line emission, are evident. This spectrum is not typical of known extragalactic objects. A uniform hot intergalactic medium of approximately 36% of the closure density of the universe would produce such a flux, although non-uniform models indicating less total matter are probably more realistic.

* NAS/NRC Research Associate

** Now with JPL

*** Now with UCSD

I. INTRODUCTION

Measurements of the spatially unresolved X-ray background (XRB) probe X-ray emission on a cosmological scale. Undoubtedly part of the XRB is due to discrete sources, similar to those already seen, but which are too distant to be spatially resolved. However previous studies (cf. Schwartz and Gursky 1974) have indicated that such emission is insufficient to account for the observed XRB unless there is substantial evolution in these sources. Thus most of the XRB may be due to truly diffuse emission mechanisms. One such diffuse mechanism, thermal bremsstrahlung from a hot intergalactic gas, has recently been discussed by Field and Perrenod (1977). Cowsik and Kobetich (1972) had previously noted that a thermal bremsstrahlung spectrum might explain a substantial portion of the XRB.

The Cosmic X-Ray Experiment[+] (A2) on the HEAO-1 spacecraft was designed to provide detailed spectral information on the XRB from $\sim$ 1/4 to $\sim$ 60 keV. This paper is restricted to > 3 keV to concentrate on extragalactic emission. These measurements allow more precise comparisons between the XRB and proposed emission mechanisms, whether due to classes of discrete sources or for truly diffuse emission.

[+]The HEAO A-2 experiment is a collaborative effort led by E. Boldt of Goddard Space Flight Center (GSFC) and G. Garmire of California Institute of Technology with collaborators at GSFC, CIT, JPL, and UCB.

Previous individual observations of the XRB covered parts of the 3 - 50 keV energy band. Consequently to obtain the 3 to 50 keV spectrum it was necessary to combine results from several fundamentally different experiments whose internal detector background could be determined

with less precision than for the A2 experiment. A qualitative picture of the spectrum emerged, but detailed features were more difficult to obtain because experiments with different internal backgrounds were being combined. At energies $\lesssim$ 15 keV, the spectrum determined with gas proportional counters was found to be well described as a power law; the measured photon spectral indices ranged from 1.4 (Boldt et al. 1969) to 1.7 (Gorenstein et al. 1969). A steeper spectrum was found (Bleeker and Deerenberg 1970; Dennis et al. 1973; Kinzer et al. 1978) with scintillators at energies $\gtrsim$ 15 keV. Scintillator observations by Schwartz and Peterson (1974) indicated such a change in the spectrum within a single experiment.

II. EXPERIMENT DESCRIPTION

We give here a brief description of the HEAO A-2 experiment which has been described in more detail by Rothschild et al. (1979). The A2 experiment scans great circles of the sky about every ½ hour. The spin axis of HEAO-1 always points toward the sun, so the entire sky is surveyed every 6 months. The experiment consists of 6 mechanically collimated multi-anode gas proportional counters; each has an area of $\sim$ 800 cm^2. We report here data from 3 of these detectors--the argon-filled Medium Energy Detector (MED) and two xenon-filled High Energy Detectors (HED1 and HED3). HED2 has not been included since it is a more conventional detector that has greater susceptibility to non X-ray background than the other two HED's. Each detector has two layers for which separate spectra have been accumulated. Figure 1 shows a cross-section of an HED.

The measurement of the XRB is based on the fact that the detector response to diffuse emission increases linearly with solid angle. For this reason each detector views the XRB through 2 fields of view

(FOV). The large FOV has a solid angle about twice that of the small FOV. One FOV for each detector is $3^0 \times 3^0$, and the other is either $3^0 \times 6^0$ or $3^0 \times 1\frac{1}{2}^0$. The XRB flux, F, is given by

$$F = \frac{(C_L - C_S) - (IB_L - IB_S)}{A\Omega_L - A\Omega_S}$$

in which C is the count rate, IB is the internal background, $A\Omega$ is the geometry factor, and the subscripts refer to the large and small FOVs. The detectors were designed so that the internal background would be the same for both FOVs. As shown in Figure 1, the differing FOV are due to mechanical collimation outside the active counter volume and signals from the different FOVs are extracted from identical wires which alternate in the same detector volume. The equality of internal backgrounds was verified prior to launch, and we have found no evidence indicating an imbalance while in orbit.

Diffuse ambient energetic electrons can also produce counting rates roughly proportional to a solid angle. Two techniques have been used to minimize this problem. First HED1 and HED3 have a particle veto layer above the X-ray detecting volume. This reduces the instrumental response to electrons by a factor of $\sim$ 100. Secondly periods of high electron intensity (as determined from anti-coincidence rates) have been excluded from the data set. These techniques have made electron contamination negligible for the data reported here.

The spectral response function has been determined for both layers of all detectors before launch by exposing the detectors to mono-energetic X-ray beams. The gain of the detectors while in orbit is calibrated using on-board radioactive sources. As a check of this procedure, the

spectrum of the Crab Nebula has been measured and is shown in Figure 2. The good agreement with previous measurements gives confidence in the spectrum measured for the XRB. The instrumental response used for the XRB includes effects due to the partial transmission of X-rays through the collimators at high energies ($\gtrsim$ 40 keV) which increases the effective solid angle of the detectors to the XRB. The size of this effect has been calculated using a computer simulation of X-ray transmission through the collimators.

III. DATA SELECTION

Each 40.96 second period of data (during which time HEAO-1 rotates $\sim 6^{0}$) must meet certain criteria to be included in this study. The selection was done independently for each detector. As noted above, periods with high ambient electron intensity were rejected. Other requirements were used to avoid effects due to our galaxy and to known point sources: 1) only regions of the sky more than 20^{0} from the galactic plane were included, 2) periods were excluded if a known X-ray source whose peak catalogued intensity is at least 5 Uhuru Flux Units (UFU) was in the detector's FOV, 3) temporal homogeniety of the detector's counting rate was required. Requirement 3) eliminates isolated point sources with observed intensities greater than $\sim$ 1 UFU.

Data presented here are from days 233 to 285 of 1977. This corresponds to regions of the sky with ecliptic longitudes either between 238^{0} and 289^{0} or between 58^{0} and 109^{0}. The total exposures for MED, HED1, and HED3 are 14, 37, and 29 m^{2}-sr-sec respectively.

IV. RESULTS

Various models are tested by comparing the observed spectrum to that produced by convolving each model's incident spectrum with

the detector response function. Parameters of a model are determined by minimizing χ^2. The fits are never acceptable in a statistical sense if only counting statistics are used. Consequently estimates of the uncertainty in the determination of parameters are based on the spread in values for different detector layers.

Previous investigators have found that the spectrum $\lesssim$ 15 keV could be adequately described as a power law with photon spectral index Γ from 1.4 to 1.7. Figure 3 shows the results of comparing power law spectra with the observations. Although a power law with Γ = 1.4 provides a good description $\lesssim$ 15 keV, the fit becomes progressively worse at higher energies. A steeper spectrum (Γ = 1.7) provides a better overall description, but is clearly unacceptable. These results confirm previous observations that a single power law is not appropriate for the energy range 3 to 50 keV.

The softening of the spectrum at high energies suggests a thermal bremsstrahlung model may be appropriate. The thermal bremsstrahlung model includes relativistic corrections to the electron-ion Gaunt factor (Quigg 1978) and electron-electron bremsstrahlung (Maxon 1972). The results for three temperatures are shown in Figure 4a. A temperature of 25 keV is clearly too cold, and 60 keV too hot. The best fit temperature is 40 $\pm$ 5 keV, and the figure shows that this model provides an excellent description of the data. Using the average normalization of the five layers, we show in Figure 4b the spectrum of the 40 keV model. The intensity of the XRB at 10 keV is 3.2 keV/keV-cm^2-sr-sec, with an estimated absolute precision of $\sim$ 10%. This intensity is consistent with the average of previous results as compiled by Schwartz and Gursky (1974).

A more detailed thermal bremsstrahlung model has been developed by Field and Perrenod (1977) in which the emission is from a hot intergalactic gas (IGG). The IGG is heated beginning at epoch z_c and cools due to expansion of the universe. Such a model produces an observed spectrum very similar to an isothermal thermal bremsstrahlung spectrum. Best fit parameters for such a model are $z_c = 3$ and a present temperature of 26 keV. These parameters are strongly anti-correlated and so are poorly determined individually. The amount of gas depends on the clumping factor, but for a uniform IGG the required density is 36% of the closure density of the universe.

There are no indications of additional spectral features--the residuals to a 40 keV model are $\lesssim$ 1% from 3 to 20 keV. Iron line emission in the universe will create an edge at the rest-frame energy of the line. The shape of the feature depends on the luminosity of the line as a function of redshift, but is approximately a step function in photon flux for uniform volume emissivity. Solar iron abundance in a hot IGG will make a $\sim$ 0.3% edge at 6.9 keV. Iron line emission from clusters of galaxies will make an edge of $\sim$ 1% at 6.7 keV assuming that there is no evolution, that the average equivalent width is 400 eV (Mushotzky et al. 1977), and that clusters comprise 8% of the XRB at 6.7 keV (see below). Preliminary analysis indicates a 90% confidence upper limit of 2% for a 6.7 keV edge.

V. DISCUSSION

The spectrum of the XRB is most simply described as due to diffuse emission from a hot gas. However, it is possible that the XRB is comprised of discrete sources whose spectra sum to approximate a 40 keV thermal spectrum. Present knowledge of the local volume emissivity

and spectra of classes of extragalactic sources does not support this possibility, and so attempts to explain the XRB as discrete sources have found it necessary to make assumptions about both the volume emissivity (or its evolution) and spectrum (or its evolution) of a class of X-ray sources.

Clusters of galaxies and Seyfert galaxies are the best studied extragalactic sources, and, assuming no evolution, appear to be the dominant discrete contributors to the XRB. N galaxies (Marshall et al. 1978), BL Lacertae objects (Schwartz et al. 1978), and QSOs (Apparao et al. 1978) have substantially lower local volume emissivities. Narrow emission line galaxies will make a small contribution (cf. Schwartz 1979), but it is not yet possible to compute a luminosity function for such objects.

For these reasons, we have included only clusters and Seyferts to compute the contribution of discrete objects to the XRB. The 2-6 keV luminosity function calculated by Schwartz (1978) for clusters and the 2-10 keV luminosity function calculated by Tananbaum et al. (1978) for Seyferts have been used. The luminosity function for Seyferts has been truncated at $10^{42.5}$ and 10^{45} ergs s^{-1} (the limits of the observed luminosities). The luminosity functions must also be consistent with source count studies and analysis of XRB fluctuations. To convert the luminosity function to a predicted source count distribution we have assumed a 3/2 power law distribution and taken 1 UFU to be 1.7 and 2.4×10^{-11} ergs s^{-1} cm^{-2} in the 2-6 and 2-10 keV bands respectively. Warwick and Pye (1978), also assuming a 3/2 power law distribution, found k, the number of sources with intensities greater than 1 UFU, to be 15 ± 3 sr^{-1}. This value is consistent with values from other analyses

of source counts and fluctuations in the XRB (cf Schwartz 1979). Since the luminosity functions produce more than enough source counts, we have reduced the normalization for clusters by 19% so that k_{CL} and k_{SEY} sum to 15. The percentage contribution to the XRB is computed as a function of energy using the typical spectrum of clusters (Mushotzky et al. 1978b) and Seyferts (Mushotzky et al. 1979) by integrating the volume emissivity out to z of 3 for a deceleration parameter q_o of zero and dividing by the observed XRB intensity. Intensities, rather than volume emissivities, are compared since the intensity is the observable and the relationship between volume emissivity and intensity depends on the shape of the source spectrum The Hubble constant is assumed to be 50 km s^{-1} Mpc^{-1}. If q_o is $\frac{1}{2}$, the contribution of discrete sources is reduced by $\sim$ 15%. Explicitly, the local volume emissivities that were used are:

$$B_{CL} = 1.14 \times 10^{38} E^{-0.4} e^{-E/6} \text{ ergs } s^{-1} \text{ Mpc}^{-3} \text{ keV}^{-1}$$

$$B_{SEY} = 1.29 \times 10^{38} E^{-0.7} \text{ ergs } s^{-1} \text{ Mpc}^{-3} \text{ keV}^{-1}$$

Using a distribution of spectral parameters (rather than typical parameters) changes the results very little. For example, assuming 25%, 50% and 25% of the 2-10 keV Seyfert luminosity is due to Seyferts with spectral indices of 0.42, 0.7, and 0.98 respectively slightly hardens the integrated intensity, but the intensity even at 50 keV is multiplied by a factor of only 1.1.

As shown in Figure 5, Seyfert galaxies contribute from 12% to 18% of the XRB for energies between 4 and 50 keV. At lower energies a wide variety of Seyfert spectra have been observed, so estimates of the contribution are necessarily uncertain as indicated by the dashed

lines. Although the spectrum of the XRB cannot be fit with the 1.7 photon power law characteristic of Seyferts, subtracting the Seyfert contribution would not substantially change the shape of the XRB spectrum since the contribution is small. The major effect would be to lower slightly the best fit temperature. The shape of the cluster contribution, however, is dramatically different than that of the XRB spectrum. Subtraction of such a large cluster component would leave a spectrum too flat at energies less than 10 keV to be well fit by a thermal spectrum. The only sources known to have such flat spectra are the BL Lacs Mkn421 and Mkn501 (Mushotzky et al. 1978a). Although data are limited, no steepening in their spectra has been observed above 10 keV as would be required to comprise the remainder of the XRB. In addition BL Lacs are estimated to contribute only $\sim$ 1% of the XRB (Schwartz et al. 1978) assuming no evolution. These difficulties suggest that the contribution of clusters has been substantially overestimated as would be the case if clusters at large redshifts were less luminous at energies > 3 keV. Such evolutionary models have been discussed by Perrenod (1978).

The above calculations indicate that for discrete sources to contribute more than $\sim$ 20% of the XRB, there must be a strongly evolving class of sources. QSOs are potentially such a class since they are known to evolve strongly at other wavelengths and are now known to be typically strong X-ray sources (Giacconi 1979). However it is difficult to estimate a priori the rate of evolution of the X-ray volume emissivity since different types of QSOs evolve very differently (Schmidt 1976). If QSOs do evolve sufficiently rapidly ($B_{QSO} \propto e^{13t}$ is sufficient assuming 3C273 is typical), then the measured spectrum of the XRB indicates that they typically have power law spectra with a photon spectral index of $\sim$ 1.4 and a steepening of their spectra at higher energies to create

an apparent temperature of $\sim$ 40 keV. This steepening in the rest frame would be at energies several times 40 keV since for QSOs to comprise the XRB the typical QSO must be at $z \gtrsim 1$.

An important test of the hypothesis that QSOs comprise the XRB is whether their spectra are similar to that of the XRB. For only one QSO, 3C273, is a broad-band spectrum available (Primini et al. 1979; Worrall et al. 1979). Its spectrum is consistent with the XRB spectrum provided that it is redshifted appropriately for $z = 2$. However, this effectively redshifts the break in the XRB spectrum to energies higher than are available for the 3C273 spectrum. It remains for future observations to determine the typical spectral index of QSO spectra, and whether they typically have a break in their spectrum near 100 keV.

Although the XRB could be comprised of a class of strongly evolving sources such as QSOs or even of a class of sources not yet discovered, the measured spectrum strongly suggests emission from a diffuse, hot gas. Field and Perrenod (1977) reviewed the observational constraints on the amount of a hot intergalactic gas (IGG). They concluded that cosmologically significant amounts of hot gas ($\Omega \lesssim 1$) could not be ruled out, although the large amount of energy required to heat the gas to 40 keV makes the existence of such gas uncertain. Clumping of the gas reduces the needed energy input and avoids possible conflicts with the existence of neutral hydrogen near the edge of galaxies (Bergeron and Gunn 1977) and between galaxies (Cowie and McKee 1976). Field and Perrenod investigated in detail one model for clumping in which the XRB is comprised of emission from isothermal, self-gravitating spheres of hot gas. They found it impossible for such a model to be consistent with both the number of point sources indicated by analysis of fluctuations

in the XRB and the observed XRB intensity. However, large spheres will substantially reduce the required number of sources (Fabian 1972), and a consistent model may be possible for spheres with radii greater than $\sim$ 50 Mpc. A study of spatial correlations in the XRB could reveal the scale size for clumping in the IGG and identify individual sources.

VI. CONCLUSION

Measurements of the spectrum of the XRB between 3 and 50 keV by HEAO-A2 are remarkably well fit by an isothermal thermal bremsstrahlung model with a temperature of 40 keV. No other spectral features are evident. This spectrum is not typical of presently resolved extragalactic sources, indicating they probably contribute a small fraction of the XRB in this energy range. Because of the limited data presently available, more observations are needed to determine if the typical spectrum of a strongly evolving class of objects (such as QSOs) is consistent with their comprising most of the XRB in the 3-50 keV energy band. Free-free emission from a clumped intergalactic medium with an apparent temperature of $\sim$ 40 keV would explain the observations. The discovery of large scale spatial correlations in the XRB could provide corraborating evidence for such emission.

REFERENCES

Apparao, K.M.V., Bignami, G.F., Maraschi, L., Helmken, H., Margon, B., Hjellming, R., Brandt, H.V., and Dower, R.G. 1978, Nature 273, 450.

Bergeron, J. and Gunn, J. 1977, Ap. J. 217, 89.

Bleeker, J. and Deerenberg, A. 1970, Ap. J. 159, 215.

Boldt, E., Desai, U., Holt, S., and Serlemitsos, P. 1969, Nature 224, 677.

Cowie, L. and McKee, C. 1976, Ap. J. 209, L105.

Cowsik, R., and Kobetich, E. 1972, Ap. J. 177, 585.

Dennis, B., Suri, A., and Frost, K. 1973, Ap. J. 186, 97.

Elvis, M., Maccaro, T., Wilson, A., Ward, M., Penston, M., Fosbury, R., and Perola, G. 1978, Mon. Not. R. Astr. Soc. 183, 129.

Fabian, A.C. 1972, Nature Phys. Sci. 237, 19.

Field, G., and Perrenod, S. 1977, Ap. J. 215, 717.

Giacconi, R. 1979, Bull. Amer. Phys. Soc. 24, 672.

Gorenstein, P., Kellog, E., and Gursky, H. 1969, Ap. J. 156, 315.

Kellogg, E., Baldwin, J., and Koch, D. 1975, Ap. J. 199, 299.

Kinzer, R., Johnson, W., and Kurfess, J. 1978, Ap. J. 222, 370.

Marshall, F.E., Mushotzky, R.F., Boldt, E.A., Holt, S.S., Rothschild, [illegible], and Serlemitsos, P.J. 1978, Nature 275, 624.

Maxon, S. 1972, Phys. Rev. A. 5, 1630.

Mushotzky, R.F., Boldt, E.A., Holt, S.S., Pravdo, S.H., Serlemitsos, P.J., Swank, J.H., and Rothschild, R.E. 1978a, Ap. J. (Letters) 226, L65.

Mushotzky, R.F., Serlemitsos, P.J., Smith, B., Boldt, E.A., and Holt, S.S. 1978b, Ap. J. 225, 21.

Mushotzky, R.F., Boldt, E.A., Holt, S.S., Marshall, F.E., and Serlemitsos, P.J., 1979, submitted to Ap. J.

Perrenod, S.C. 1978, Ap. J. 226, 566.

Primini, F.A. et al. 1979, Nature 278, 234.

Quigg, C. 1968, Phys. Fluids 11, 461.

Rothschild, R.E. et al. 1979, Space Sci. Instr., in press.

Schmidt, M. 1978, Physica Scripta 17, 329.

Schwartz, D A. 1978, Ap. J. 220, 8.

Schwartz, D A. 1979, Proc. of the XXI COSPAR/IAU Symposium in X-Ray Astro, Pergamon Press, in press.

Schwartz, D A., Bradt, H.V., Doxsey, R.E., Griffiths, R.E., Gursky, H., Johnston, M., and Schwarz, J. 1978, Ap. J. (Letters) 224, L103.

Schwartz, D., and Gursky, H. 1974, in X-Ray Astronomy, ed. by R. Giacconi and H. Gursky.

Schwartz, D., and Peterson, L. 1974, Ap. J. 190, 297.

Tananbaum, H., Peters, G., Forman, W., Giacconi, R., Jones, C., and Avni, Y. 1978, Ap. J. 223, 74.

Warwick, R.S., and Pye, J.P. 1978, MNRAS 183, 169.

Worrall, D.M., Mushotzky, R.F., Boldt, E.A., Holt, S.S., and Serlemitsos, P.J. 1979, Ap. J. , in press.

FIGURE CAPTIONS

Figure 1 - A cross-section of HED1 showing the collimator, the particle anti-coincidence layer, the first xenon layer (M1), the second xenon layer (M2), and the bottom veto layer. The extreme left and right cells of M1 and M2 are also in anti-coincidence. Odd anodes of M1 are connected together and view the sky through 3^0 x 3^0 collimator tubes. Even anodes view the sky through 3^0 x 6^0 tubes. The anodes of M2 are connected in the same fashion. HED3 is identical except the 3^0 x 6^0 tubes are replaced by 3^0 x $1\frac{1}{2}^0$ tubes. The argon-filled MED is similar to HED3, but has a Be entrance window and no particle anti-coincidence layer.

Figure 2 - The ratio as a function of energy of the observed counts from the Crab Nebula to the counts predicted by convolving with the detector response function an absorbed power-law incident spectrum. Different symbols are used to represent the first layer of the MED and both layers of HED1 and HED3. Statistical errors are indicated when larger than the size of the symbols.

Figure 3 - The ratio of the observed counts for the XRB to that predicted for power-law incident spectra. Statistical errors are shown when larger than the size of the symbols.

Figure 4 - a) The ratio of the observed counts for the XRB to that predicted for thermal bremsstrahlung incident spectra. Statistical errors are shown when larger than the size of the symbols.

b) The incident spectrum for the 40 keV model. The mean of the normalizations for the 5 independent layers shown in a) has been adopted with an estimated absolute accuracy of $\sim$ 10%.

Figure 5 - The fractional contribution of clusters of galaxies and Seyfert galaxies to the XRB. The normalizations (k) of the source count distribution, the luminosity function, and the source spectrum (B(E)) used in the calculation are also indicated. k is the number of sources per steradian whose intensity is greater than 1 UFU. The luminosity, L, is in units of 10^{44} ergs s^{-1} in the 2-6 keV band for clusters and the 2-10 keV band for Seyferts.

Authors' Addresses:

E.A.Boldt, S.S.Holt, F.E.Marshall, R.F.Mushotzky, L.A.Rose, and
P.J.Serlemitsos
Code 661
NASA Goddard Space Flight Center
Greenbelt, Md. 20771

R. Miller
Jet Propulsion Laboratory
4800 Oak Grove Drive
Pasadena, CA 91103

R.E.Rothschild
Mail Code C011
University of California at San Diego
La Jolla, CA 92093

ORIGINAL PAGE IS
OF POOR QUALITY

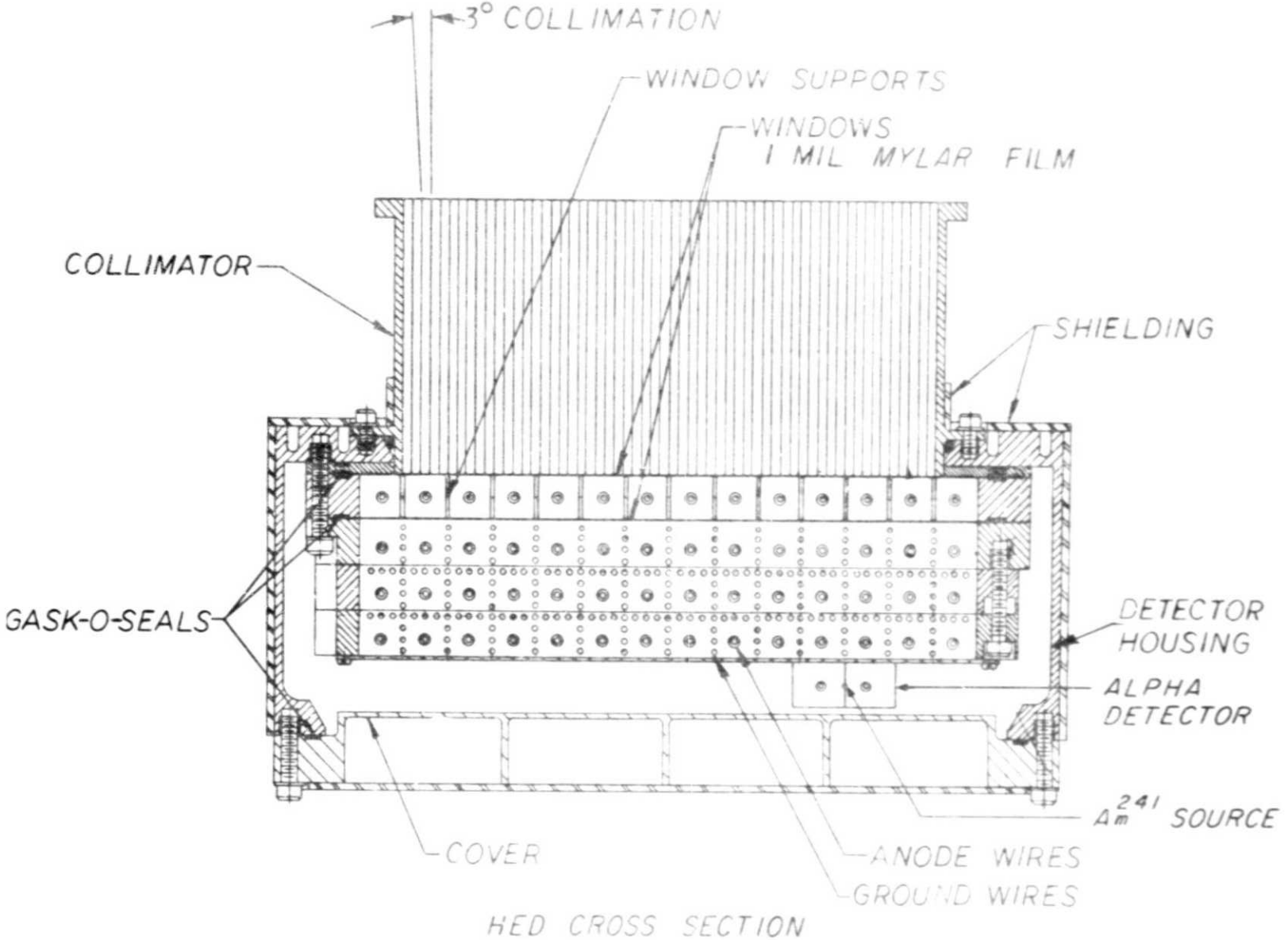

HED CROSS SECTION

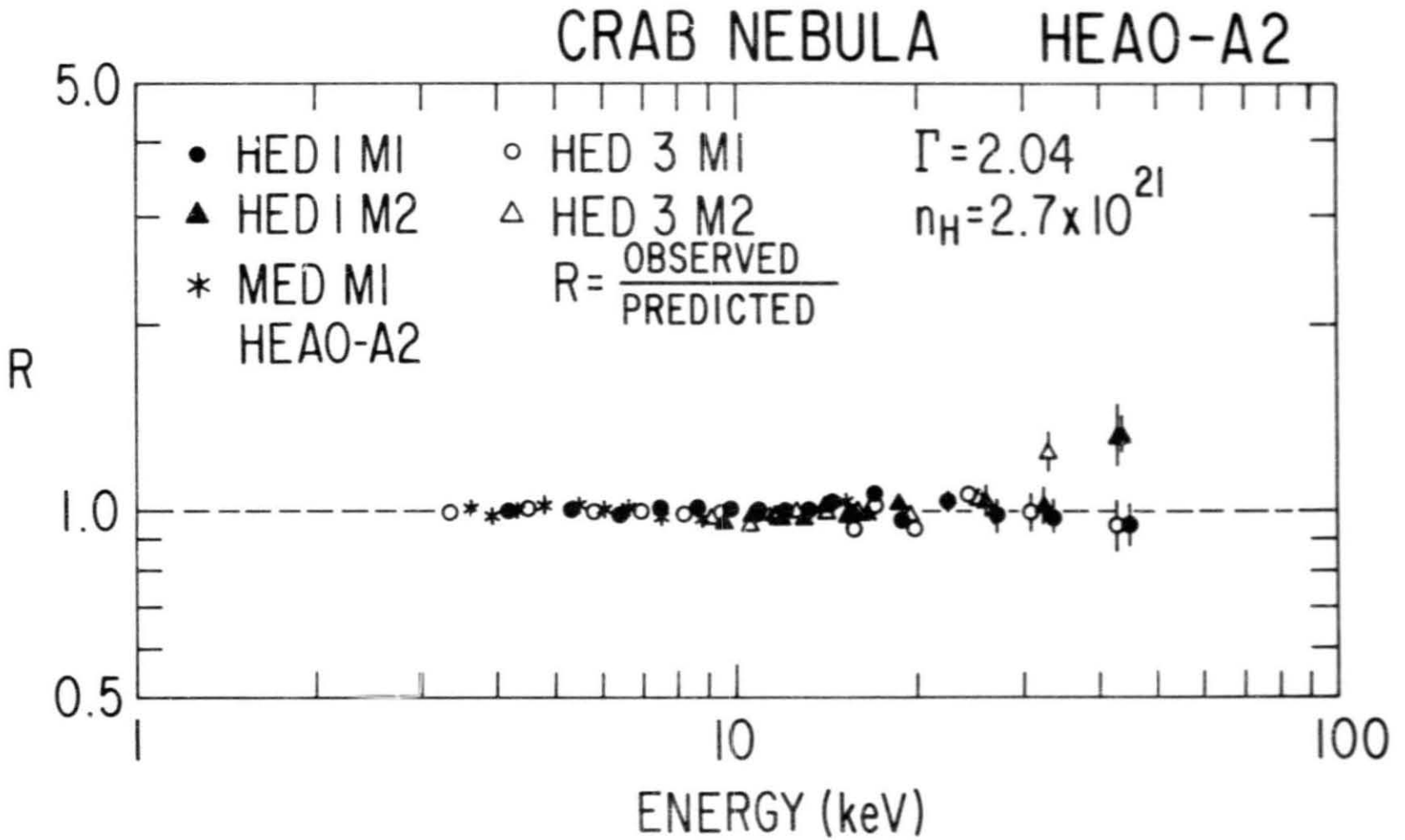
CRAB NEBULA HEAO-A2
5.0
1.0
0.5
R
1
10
100
ENERGY (keV)
HED 1 M1
HED 1 M2
MED M1
HEAO-A2
HED 3 M1
HED 3 M2
R = OBSERVED / PREDICTED
Γ = 2.04
$n_H = 2.7 \times 10^{21}$

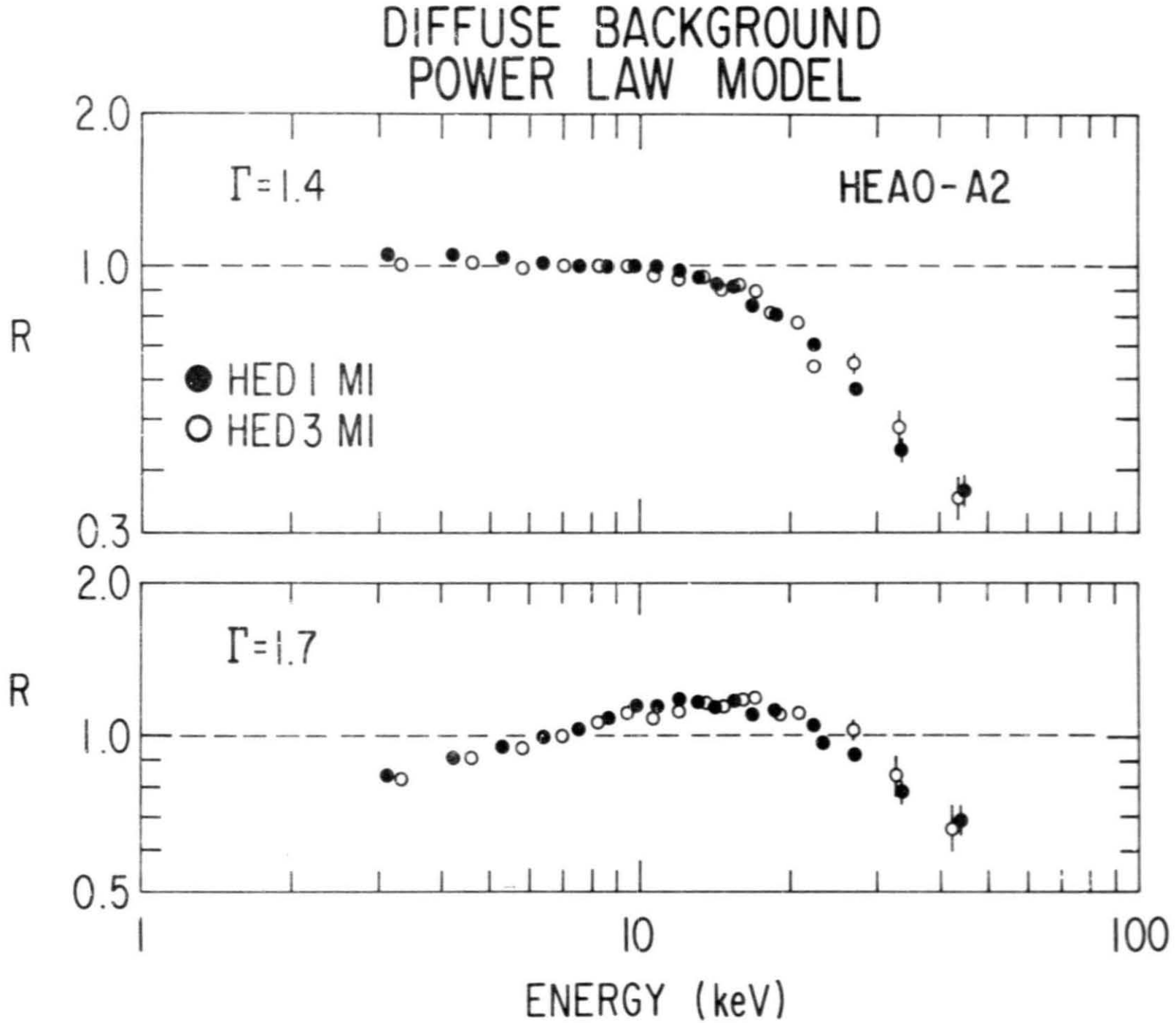
DIFFUSE BACKGROUND
POWER LAW MODEL
Γ=1.4
HEAO-A2
HED 1 MI
HED 3 MI
Γ=1.7
R
2.0
1.0
0.3
0.5
1
10
100
ENERGY (keV)

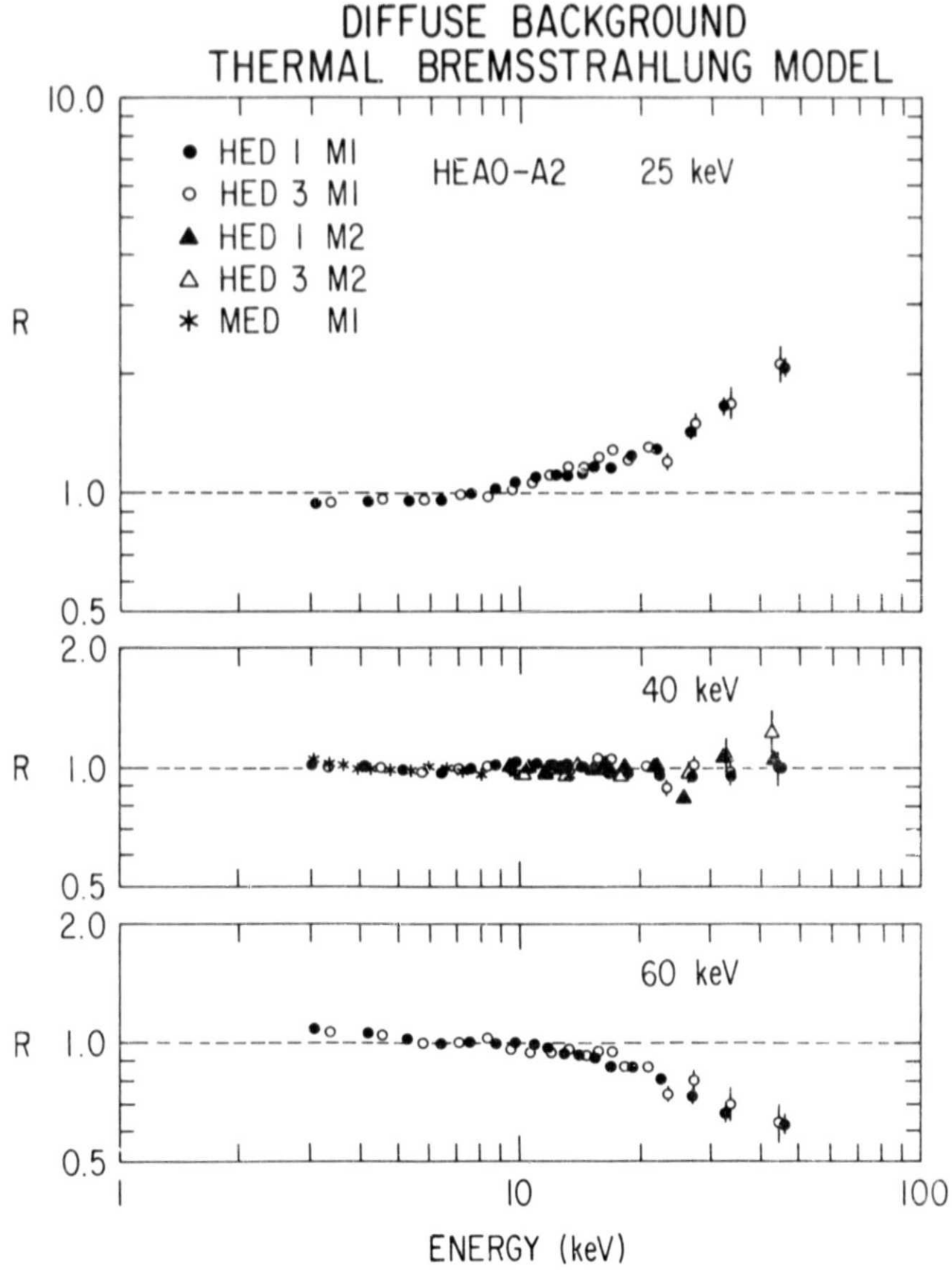
DIFFUSE BACKGROUND
THERMAL BREMSSTRAHLUNG MODEL
HED 1 M1
HED 3 M1
HED 1 M2
HED 3 M2
MED M1
HEAO-A2
25 keV
40 keV
60 keV
R
10.0
1.0
0.5
2.0
1
10
100
ENERGY (keV)

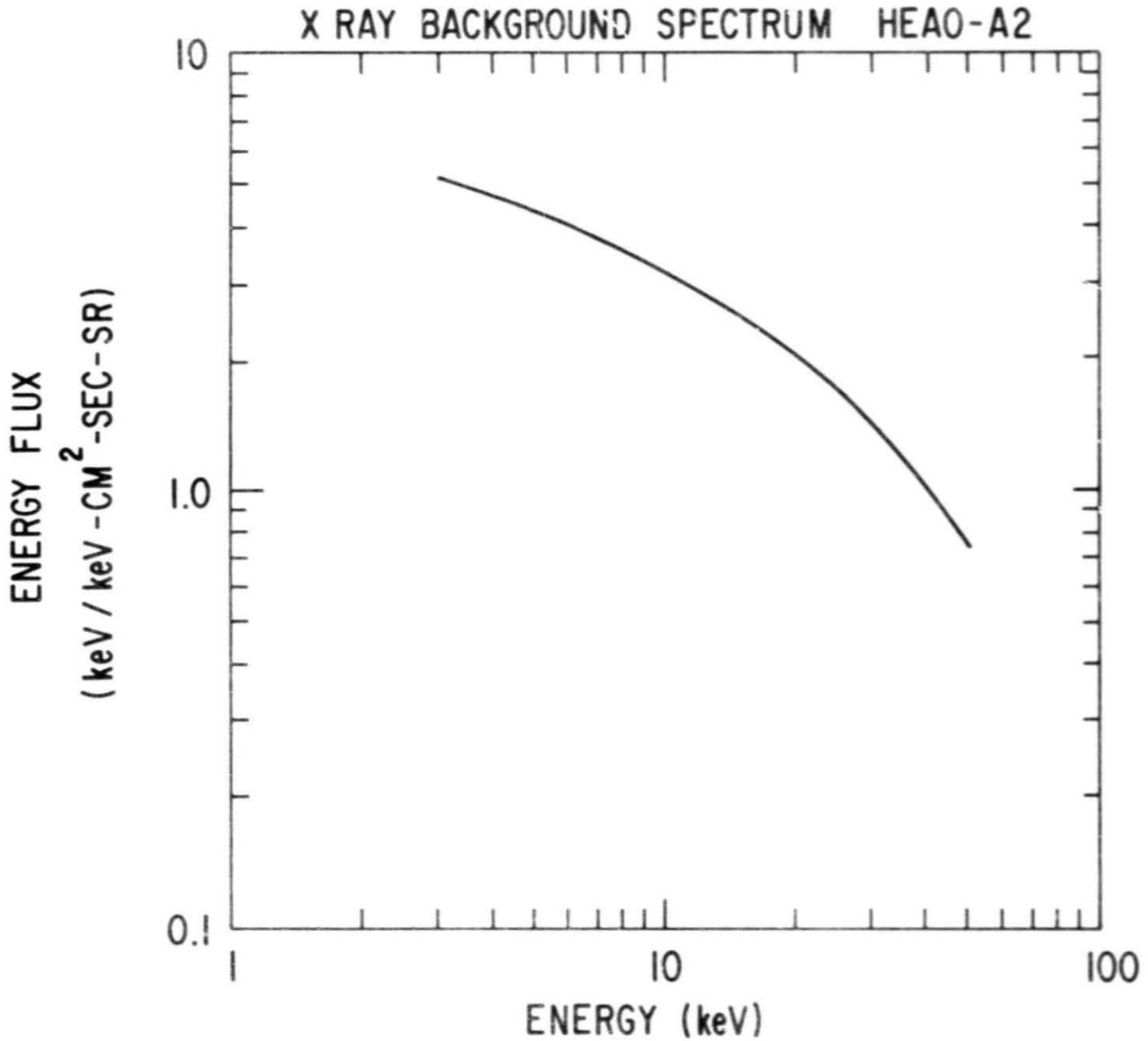
X RAY BACKGROUND SPECTRUM HEAO-A2
ENERGY FLUX
(keV / keV-CM^2-SEC-SR)
10
1.0
0.1
1
10
100
ENERGY (keV)

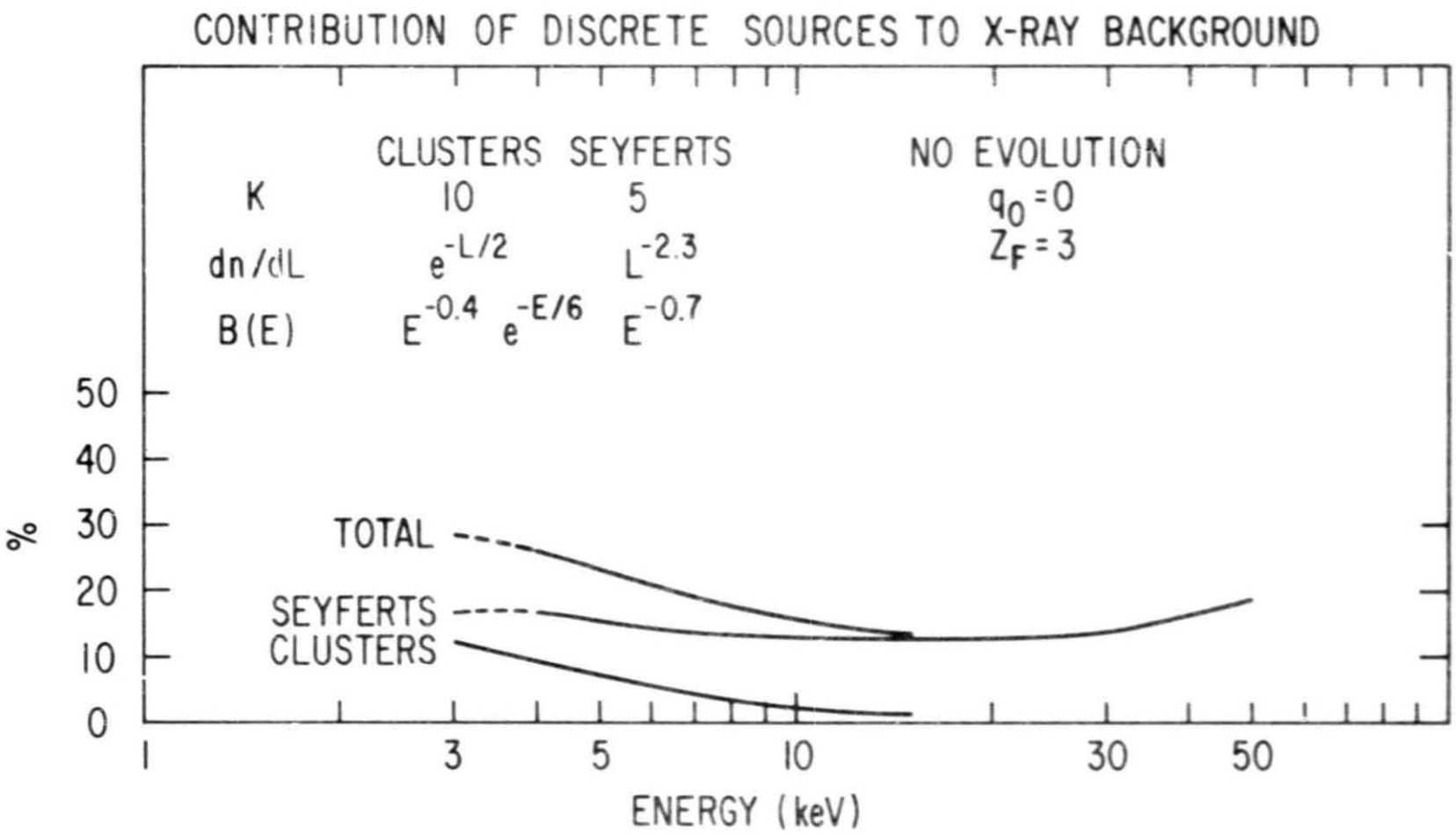
CONTRIBUTION OF DISCRETE SOURCES TO X-RAY BACKGROUND
CLUSTERS SEYFERTS
K 10 5
dn/dL $e^{-L/2}$ $L^{-2.3}$
B(E) $E^{-0.4}$ $e^{-E/6}$ $E^{-0.7}$
NO EVOLUTION
$q_0 = 0$
$Z_F = 3$
TOTAL
SEYFERTS
CLUSTERS
%
50
40
30
20
10
0
1
3
5
10
30
50
ENERGY (keV)